Structure and fluctuations of phosphatidylcholines in the vicinity of the main phase transition

G. Pabst,[1,*] H. Amenitsch,[1] D. P. Kharakoz,[2] P. Laggner,[1] and M. Rappolt[1]
[1]*Institute of Biophysics and X-Ray Structure Research, Austrian Academy of Sciences, Schmiedlstraße 6, 8042 Graz, Austria*
[2]*Institute of Theoretical and Experimental Biophysics, Russian Academy of Sciences, Pushchino, Moscow Region, 142292 Russia*
(Received 21 January 2004; revised manuscript received 5 April 2004; published 19 August 2004)

We have determined the structural properties and bending fluctuations of fully hydrated phosphatidylcholine multibilayers in the fluid (L_α) phase, as well as the structure of the ripple ($P_{\beta'}$) phase near the main phase transition temperature (T_M) by x-ray diffraction. The number of carbons, n_{HC}, per acyl chain of the studied disaturated lipids varied from 14 to 22. All lipids exhibit a nonlinear increase of the lamellar repeat distance d in the L_α phase upon approaching T_M, known as "anomalous swelling." The nonlinear increase reduces with chain length, but levels off at a constant value of about 0.5 Å for lipids with more than 18 hydrocarbons per chain. A detailed analysis shows that anomalous swelling has two components. One is due to an expansion of the water layer, which decreases with chain length and finally vanishes for $n_{\mathrm{HC}}>18$. The second component is due to a bilayer thickness increase, which remains unchanged in its temperature dependence, including a nonlinear component of about 0.5 Å in the vicinity of T_M. Thus, anomalous swelling above 18 hydrocarbons per chain is due to the pretransitional effects on the membrane only. These results are supported by a bending fluctuation analysis revealing increased undulations close to T_M only for the short chain lipids. We have further calculated the electron density maps in the ripple phase and find no coupling of the magnitude of the ripple amplitude to the chain length effects observed in the L_α phase. Hence, in agreement with an earlier report by Mason *et al.* [Phys. Rev. E **63**, 030902 (2001)] there is no connection between the formation of the ripple phase and anomalous swelling.

DOI: 10.1103/PhysRevE.70.021908 PACS number(s): 87.16.Dg, 87.64.Bx, 87.15.Ya, 05.70.Fh

I. INTRODUCTION

Model membranes composed of phospholipid species are well recognized for many biological and technological aspects. One of the most disputed but still not fully understood fundamental issues concerns the physics of the main phase transition of phosphatidylcholines (PCs), which is driven by a change of the hydrocarbon chain conformation from an all-*trans* to a *trans-gauche* state. Below the main phase transition temperature T_M, many phosphatidylcholines exhibit a lamellar phase with in-plane regularly spaced ripples, denoted as the $P_{\beta'}$ phase [1,2]. Above T_M the lipid-water system is in the lamellar L_α phase, which is characterized by strong collective bilayer fluctuations and a vanishing shear modulus. The L_α phase is considered to be the biologically most relevant phase.

Both phases L_α and $P_{\beta'}$, respectively, have been studied extensively over recent decades. However, a microscopic understanding of both structures and their changes with temperature especially in the vicinity of T_M is a matter of ongoing research. Even with good electron density maps [3,4] the conformations of the lipids in the ripple phase are still uncertain. One view that is consistent with structural studies [3,5] is that the ripples are related to the coexistence of alternating fluid and gel domains, and various theories have been proposed to rationalize this model [6]. In contrast, it has been suggested [4] that the ripple phase can consist entirely of gel-state lipid molecules. Further, a metastable ripple phase is often seen when the system is cooled into the ripple phase from the L_α phase [7], for which an electron density map has been reported only very recently [8]. Finally, PCs with 17 hydrocarbons per chain and above were found to exhibit a so-called submain transition slightly below T_M, in which parts of the chain packing were found to become fluid, L_α-like [9,10].

We focus primarily on the changes of the structural and mechanical properties of the L_α phase as a function of temperature close to T_M. Here, many studies have reported a nonlinear increase of the lamellar repeat distance d upon lowering the temperature toward T_M [11–21]. Furthermore, other membrane parameters, e.g., the bilayer permeability [22,23], heat capacity [24], fluorescence lifetime [25], NMR order parameter [26], or ultrasound velocity [27], were also found to exhibit anomalous behavior in this regime. All these effects can be understood basically by increased density fluctuations as the system approaches the transition temperature [28,29]. It was suggested [27,30] that these density fluctuations may be an intrinsic bilayer property and that the transition is weakly but pure first order. However, it has also been argued that these fluctuations may be due to the vicinity of a second-order transition, which is preempted by a first-order one [31,32].

So far, consensus appears to have been reached only on the effect of the fluctuations on the global physical properties of the multibilayer systems: The density fluctuations in the vicinity of T_M lead to a reduction of the bilayer bending rigidity [30,33–35], which we have confirmed recently by x-ray diffraction [21]. This causes increased thermal bilayer undulations, which lead to an expansion of the interstitial water layer [12,21] due to enhanced steric repulsion of adjacent bilayers [36]. In our previous study on dimyristoyl

*Author to whom correspondence should be addressed. FAX: +43 316 4120 390. Email address: Georg.Pabst@oeaw.ac.at

phosphatidylcholine (DMPC) we found that this effect dominates the nonlinear increase of d [21]. However, there is also a small but significant nonlinear contribution from the hydrocarbon chains of about 0.5 Å [21], also reported from NMR measurements [16,26].

Deeper knowledge of the individual contributions to anomalous swelling from systematic studies on a homologous series of different chain-length lipids is still largely lacking. Several studies have reported an enhancement of the pretransitional effects upon decreasing the chain length [14,18,26,29], although a most recent study shows a break in this trend for dilauroyl phosphatidylcholine (DLPC) [37]. From an earlier study by Lemmich *et al.* [14] on perdeuterated DMPC and dipalmitoyl phosphatidylcholine (DPPC) it is known that the bilayer repulsion decreases as the chain length is increased. It is not clear, however, whether this trend extends to longer-chain lipids. If so, we expect that the anomalous swelling vanishes at a certain chain length. It is also not clear how the nonlinear component of the bilayer thickening in the vicinity of T_M depends on chain length.

In the present paper, we report x-ray diffraction studies as a function of temperature and hydrocarbon chain length of disaturated phosphatidylcholine multilamellar dispersions. Consistent with earlier studies [14,18], we find that the amplitude of anomalous swelling reduces at chain lengths in the range of 14 to 18 hydrocarbons per chain. For longer chain lipids, however, the swelling amplitude does not reduce further but exhibits a constant nonlinear component of about 0.5 Å. Decomposition of d into the membrane thickness d_B and water layer thickness d_W shows that the contribution to anomalous swelling by the water layer expansion reduces with increasing chain length and finally vanishes above 18 hydrocarbons per chain. In agreement with this result we find a sudden increase of bending fluctuations in the vicinity of T_M only for phospholipids with less than 19 hydrocarbons per chain. In contrast, the increase of the membrane thickness with decreasing temperature, and in particular its nonlinear component, in the vicinity of T_M of about 0.5 Å does not depend on the chain length. Thus, the nonvanishing pretransitional swelling of the long-chain lipids is caused by the bilayer thickening.

In view of an earlier report on the possible coupling of anomalous swelling to the formation of the $P_{\beta'}$ phase [20], we have computed the electron density maps of fully hydrated DMPC, DPPC, and diarachidoyl phosphatidylcholine (DAPC) in the ripple phase. From the low-resolution maps we have derived the magnitude of the ripple amplitude, which increases as a function of chain length. This dependence correlates neither to the available water spacing nor to its relative increase in the very vicinity of T_M approaching the transition from above. Hence, in agreement with Mason *et al.* [20], in our work the formation of the ripple phase occurs independently of anomalous swelling. Further, complementary to Ref. [20] we show that the ripple phase forms even if there is no increase of the water spacing just above T_M.

II. MATERIALS AND EXPERIMENTAL METHODS

A. Sample preparation

1,2-dimyristoylphosphatidylcholine (14:0), 1,2-dipalmitoylphosphatidylcholine (16:0), 1,2-distearoylphosphatidylcholine (DSPC, 18:0), 1,2-dinonadecanoylphosphatidylcholine (DNPC, 19:0), 1,2-diarachidoylphosphatidylcholine (20:0), and 1,2-dibehenoylphosphatidylcholine (DBPC, 22:0) were purchased from Avanti Polar Lipids (Alabaster, AL) and used without further purification. Dispersions of fully hydrated multilamellar lipid vesicles were prepared by dissolving weighted amounts of lipid in an organic solvent of $CHCl_3$-CH_3OH (2:1, v/v). The solvent was removed by placing the sample first under a stream of N_2 and subsequently under vacuum for 12 h. This yielded a dry lipid film on the bottom of the glass vial, which was rehydrated using double-distilled–deionized water to obtain samples of 25 wt % lipid. Complete hydration of the samples was achieved by keeping the samples at least 10 K above the main transition temperature and applying intermittent vigorous vortex mixing. Further annealing of the samples was achieved by repeating three times a heating-cooling cycle through the main phase transition. Samples prepared in this way display a narrow melting transition of 0.12 K– 0.18 K (full width at half maximum) as was verified by independent calorimetric measurements (scan rate 0.1 K/min, data not shown). Thin-layer chromatography tests carried out before and after experimentation showed no signs of sample degradation.

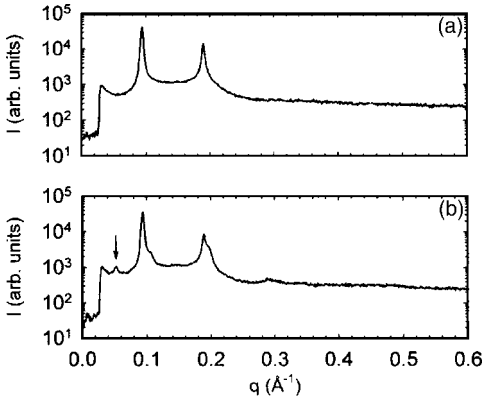

FIG. 1. Diffraction patterns of DMPC at 297.2 K (a) in the L_α phase and at 296.9 K (b) in the $P_{\beta'}$ phase (T_M=297.0 K). The ripple phase is easily identified by the in-plane ripple spacing of about 118 Å (indicated by arrow).

B. X-ray measurements

Diffraction studies were carried out at the Austrian small-angle x-ray scattering (SAXS) beamline [38,39] (Sincrotrone Trieste, Italy) using a one-dimensional position sensitive detector [40], which covered the q range ($q=4\pi \sin\theta/\lambda$) between 0.03 and 0.6 Å^{-1} at a photon energy of 8 keV. Recording the scattered intensity over a broad q range has the advantage that the phase of the lipid-water system can be inferred immediately by visual inspection of the diffraction patterns. In this way it is simple to discern L_α phase diffraction patterns from $P_{\beta'}$ phase patterns (Fig. 1). Only L_α phase diffraction patterns were considered for applying the full q-range data analysis [41] (see below). Silver behenate (d =58.38 Å [42]) was used as a standard to calibrate the angular dependence of the scattered intensity. The instrumental

resolution was determined to have a full width at half maximum of $\delta q = 2.2 \times 10^{-3}$ Å^{-1}.

For measurements, the liposomal dispersions were kept in thin-walled, 1-mm-diameter quartz glass capillaries, which were placed in a sample holder block of brass. The entry and exit windows of the sample holder were covered with a thin polymer film in order to avoid any convection due to the surrounding environment. The polymer films were tested to give no contribution to the measured intensities. The temperature of the sample was controlled with a water bath to within ±0.1 K and measured with a Pt-100 resistance temperature detector placed in the vicinity of the capillary. The samples were equilibrated for 10 min at each temperature prior to exposure. The capillaries were horizontally shifted by 1 mm to an unexposed portion of the sample after every second measurement in order to avoid radiation damage. Samples were exposed to x rays typically between 2 and 3 min. In the vicinity of T_M the temperature steps were 0.2 K, i.e., the transition midpoint could be determined with a precision of 0.1 K.

C. Data analysis

1. Fluid phase

The scattered intensities of the L_α phase diffraction patterns were corrected for detector efficiency and background noise originating from the sample cell and water. The corrected diffraction patterns were then analyzed by a previously developed algorithm [41], which models the scattered intensity

$$I(q) = \frac{S(q)|F(q)|^2}{q^2} \tag{1}$$

in the full q range. The structure factor of a single domain consisting of N bilayers is given by the modified Caillé theory [43]

$$S_L(q) = N + 2\sum_{k=1}^{N-1} (N-k)\cos(kqd) \times \exp\left\{ -\left(\frac{d}{2\pi}\right)^2 q^2 \eta [\gamma + \ln(\pi k)] \right\}, \tag{2}$$

and is averaged over a domain size distribution according to Refs. [44,45] in order to obtain $S(q)$. Further parameters appearing in Eq. (2) are the Caillé parameter η, and Euler's constant $\gamma(=0.5772\ldots)$. η is a measure of the bilayer fluctuations that depend on the bending rigidity and the bulk modulus of compression [46]. The Caillé parameter determines the shape of the long power tails of the quasi-Bragg reflections by $I(q-q_h) \propto (q-q_h)^{-(1-\eta_h)}$, where h is the lamellar diffraction order and $\eta_h \approx \eta_1 h^2$. We obtain η by a global fit of the diffraction pattern, including all Bragg reflections plus diffuse scattering. η therefore has to be regarded as an effective parameter.

The second function appearing in Eq. (1) is the form factor $F(q)$, calculated by the Fourier transform of the electron density model, which we define as the sum of three Gaussians, two centered at the electron-dense headgroups and one with negative amplitude at the methyl terminus of the hydrocarbon chains [21,41].

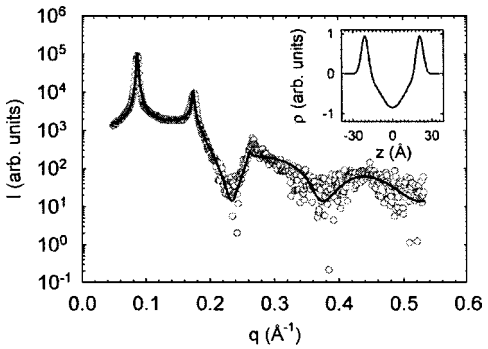

FIG. 2. X-ray diffraction pattern of fully hydrated DAPC multilamellar vesicles at 349.7 K. The data exhibit three quasi-Bragg peak reflections plus diffuse background scattering which becomes dominant at higher scattering angles and is due to the variation of the form factor with q. The pattern has been fitted in the full q range according to Eq. (1). The fit shows a good agreement with the experimental data over four orders of magnitude in intensity. The inset gives the corresponding electron density profile.

Figure 2 gives an example of the fit to our data. From the fits of our model we directly determine the lamellar repeat spacing d and the Caillé fluctuation parameter η. $d = d_B + d_W$ is then further decomposed into the membrane thickness d_B and the thickness of the interstitial water region d_W. However, this is not trivial because of the low resolution of the electron density profile (Fig. 2). Nevertheless, the correct quantitative values are, in this case, less important than their dependence on temperature and their correlation with η. Therefore, as argued in detail before [21], we define

$$d_B = 2(z_H + 2\sigma_H), \tag{3}$$

which cuts the probability distribution of the choline group near its half value [47] and is therefore an estimate for the steric bilayer thickness [48]. z_H is the position of the headgroup Gaussian with respect to the bilayer center and σ_H is its width.

The membrane thickness can be further subdivided into the hydrocarbon chain length d_C and the headgroup thickness d_H. We have demonstrated before that d_C follows essentially the temperature dependence of d_B, meaning that d_H remains constant with temperature [21]. Thus, it is sufficient to restrict ourselves to determining d, d_B, d_W, and η. For the experimental data of DAPC at 349.7 K shown in Fig. 2 we get $d = 71.7 \pm 0.1$ Å, $d_B = 52.5 \pm 0.4$ Å, $d_W = 19.2 \pm 0.4$ Å, and $\eta = 0.093 \pm 0.002$.

2. Ripple phase

In contrast to the above described treatment of the L_α phase, only the corrected intensities of the Bragg reflections were used to construct low-resolution electron density maps (EDMs) of the stable ripple phase. No particular scattering theory is considered to describe the shape and the width of the Bragg peaks. The shape of the peaks is in good approximation given by Lorentzian distributions (see below) and the width is mainly determined by the finite scattering domain

size. Since the systems are not oriented with respect to a solid substrate, unlike those described in Ref. [49], the observed patterns are powder averaged leading to an overlapping of reflections. Moreover, in contrast to previous studies on unoriented PCs [2,3] the systems were not restricted in their water content. This leads to an additional overlapping of Bragg reflections. Only those reflections which could be unambiguously indexed were used to construct the EDMs. The procedure applied is described below; it yielded EDMs of sufficient resolution to obtain robust estimates on the lengths of the short and long ripple arms, as well as the ripple amplitude.

The ripple phase, on a macromolecular level, constitutes a two-dimensional oblique crystal lattice [1–3,50], which belongs to the centrosymmetric plane group $p2$ [51]. Thus, the cell parameters a, b, and γ define the positions of the Bragg reflections in reciprocal space by [52]

$$q_{hk} = 2\pi \sqrt{\frac{h^2b^2 + k^2a^2 - 2hkab\cos(\gamma)}{a^2b^2\sin^2(\gamma)}}, \tag{4}$$

where h and k are the Miller indices. We have therefore calculated the cell parameters from the q_{hk}'s determined by fitting of Lorentzian distributions to the observed Bragg reflections

$$I_{hk}(q) = \frac{1}{q^2}\left\{\frac{2A_{hk}w_{hk}}{\pi[4(q-q_{hk})^2 + w_{hk}^2]}\right\}, \tag{5}$$

where w_{hk} is the peak width. The square root of the amplitudes A_{hk} gives the absolute value of the form factors F_{hk} needed to construct the EDMs on a relative scale by

$$\rho(x,z) = \sum_{h\geqslant 0}\sum_{k} F_{hk}\cos\left(q_x^{hk}x + q_z^{hk}z\right), \tag{6}$$

with $q_x^{hk} = 2\pi h\sin(\gamma)$ and $q_z^{hk} = 2\pi[ka/b - h\cos(\gamma)]$. In order to determine the corresponding phase, i.e., the sign of F_{hk}, we applied simple pattern recognition procedures as described in [50] to discard unreasonable EDMs, and additionally calculated the fourth moment [53]

$$\langle(\Delta\rho)^4\rangle = \frac{\sum_{hk}\left|\sum_{h'k'} F_{h'-h,k'-k}F_{h',k'}\right|^2}{\left(\sum_{hk}|F_{hk}|^2\right)^2} \tag{7}$$

for all remaining phase combinations. $1/\langle(\Delta\rho)^4\rangle$ is a measure of the "smoothness" of the EDM. Accordingly, we choose the phase combination yielding the lowest $\langle(\Delta\rho)^4\rangle$. We note, that this combined method works only for low-resolution data. For data sets with higher resolution (including reflections up to the fourth order), a phase determination by EDM models [3,8] is the better choice.

III. RESULTS AND DISCUSSION

A. Chain length dependence of swelling amplitude

Figure 3 presents our results for the d values as a function of temperature and hydrocarbon chain length. In order to show the data on a single graph, the temperature has been shifted by subtracting the respective T_M's. Clearly, all bilayer systems studied show a swelling, when T_M is approached. The deviation from a linear increase in d toward T_M is most pronounced for the shortest-chain lipid studied (DMPC). This agrees well with a previous study that reports an increase in pretransitional swelling when the length of the hydrocarbon chains is decreased [18], where the number of hydrocarbons per chain was varied from 13 to 16. Our data exhibit a swelling also for DAPC, i.e., 20 hydrocarbons per chain (Fig. 3). However, its amplitude is greatly reduced as clearly observed in Fig. 4, where we have plotted the anomalous component Δd_{an} as a function of chain length to give an approximate characterization of the swelling.

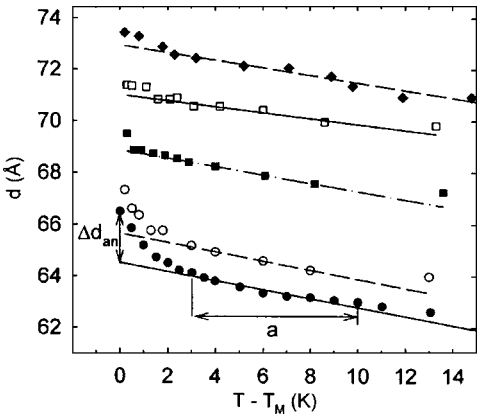

FIG. 3. Lamellar repeat distance d for various PCs as a function of temperature difference with respect to T_M. The symbols correspond to data from the following lipids: (●) DMPC ($T_M \sim 297$ K); (○) DPPC ($T_M \sim 314$ K); (■) DSPC ($T_M \sim 328$ K); (□) DNPC ($T_M \sim 333$ K), and (◆) DAPC ($T_M \sim 341$ K). Δd_{an} is the amplitude of anomalous swelling, which is given by the deviation of $d(T - T_M)$ from a straight line, obtained by a linear regression in the temperature interval from $T - T_M = 3$ to 10 K.

Δd_{an} is estimated as follows. As in our previous report [21], we take the linear component of the swelling to be "normal." Such a linear increase of d is also observed for phosphatidylethanolamines (PEs) [20], known to show no pretransitional swelling. Moreover, the slope of $d(T)$ for PEs is the same as that of $d_B(T)$ for DMPC [21]. Everything

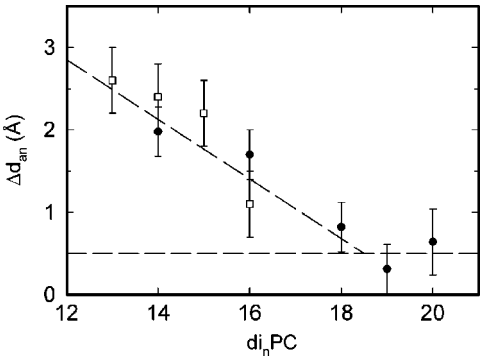

FIG. 4. Chain-length dependence of anomalous swelling component Δd_{an}. The ●'s correspond to present data, the □'s to data by Korreman and Posselt [18].

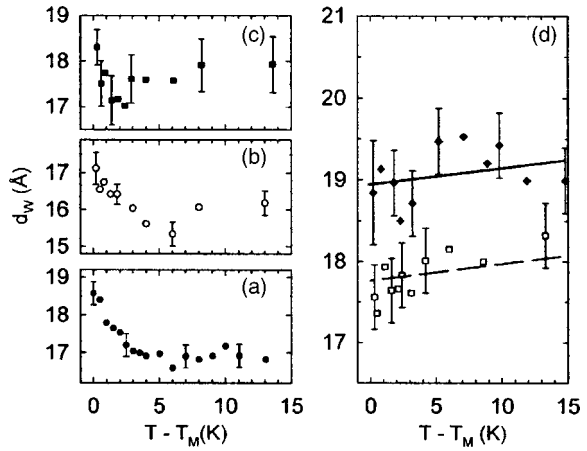

FIG. 5. Temperature dependence of the water layer thickness d_W for DMPC (a), DPPC (b), DSPC (c). (d) shows the dependencies for DNPC (□) and DAPC (♦). Lines are drawn to guide the eye. d_W increases near T_M for all lipids in panels (a)–(c), but remains roughly constant for DNPC and DAPC (d).

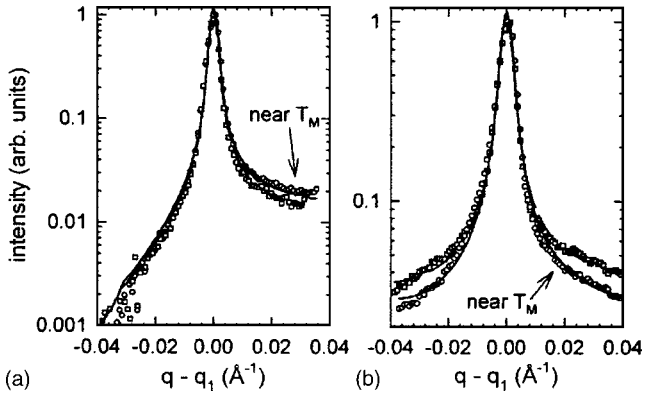

FIG. 6. First-order quasi-Bragg reflections of DMPC and DAPC. Panel (a) shows DMPC at 297 K (○) and 303 K (□) and panel (b) DAPC at 341 K (○) and 353 K (□). Solid lines show the fits of the Caillé theory structure factor to the data. The scattered intensities have been normalized to a peak value of 1. The data clearly show increased fluctuations in the vicinity of T_M for DMPC, which is not observed for DAPC (cf. Fig. 10 below).

above the linear trend close to T_M then contributes to anomalous swelling. With this definition we determine the "normal" component of the swelling by a linear regression in the temperature range T_M+3 K to T_M+10 K (Fig. 3). The lower limit of the interpolation range is set to be safely outside the pretransitional swelling regime. The upper limit is arbitrarily set to $T-T_M=10$ K. This upper limit is needed because d increases again at higher temperatures [54]. The linear regression is then extrapolated to T_M and the difference of the last d value from this line gives Δd_{an} [55]. Results are shown in Fig. 4, which also contains data that we have estimated from the results of Korreman and Posselt [18]. While the swelling, as stated above, decreases with chain length, it does not vanish completely, but remains constant, above 18 carbons/chain at about 0.5 Å.

B. Bilayer separation and fluctuations

In order to be able to attribute the chain-length dependence of Δd_{an} to the nonlinear increase of either d_B or d_W, we have analyzed the diffraction data in terms of the global model described in the material and methods section. The temperature dependence of d_W is shown in Fig. 5. Panels (a)–(c) show the data for DMPC, DPPC, and DSPC, for which d_W, upon approaching T_M, first remains constant or slightly decreases and then increases suddenly a few degrees above T_M. Although, given the experimental uncertainty, it is difficult to quantify the extent of the water layer expansion, it clearly decreases from about 1.5 Å for DMPC to about 1.0 Å for DSPC. In contrast, the d_W results for DNPC and DAPC, presented in Fig. 5(d), show no significant dependence on temperature.

There is an obviously nonmonotonic variation of d_W with chain length at a fixed $T-T_M$. The bilayer separation for fully hydrated bilayers in the L_α phase is a delicate balance between attractive and repulsive forces. Hence, any small perturbation of the system due to, for example defects induced by small differences in preparation and/or thermal histories, may play a role. Several samples were prepared and measured a second time, showing a variation of d at a given temperature by about 1 Å. This agrees with findings by Nagle and Tristram-Nagle, who report a variation of d for nominally equal samples by almost 3 Å for hitherto unclear reasons [47]. Nevertheless, as long as the samples are nominally fully hydrated there are no effects on the magnitude of pretransitional swelling [56]. Thus, with respect to the temperature dependence of d_W only relative changes are of significance. In contrast, the membrane thickness should depend on the chain length in a meaningful way (see below).

The results on d_W can be cross checked by an analysis of the bending fluctuation parameter η: The expansion of d_W in the vicinity of T_M is driven by steric repulsion due to increased undulations as verified for DMPC [21]. Hence, because of our results on d_W, we expect to detect increased fluctuations only for lipids with fewer than 19 hydrocarbons per chain.

Because of the power law behavior of the quasi-Bragg peaks, increased fluctuations will show up as increased scattered intensity in the tails of the relections. Figure 6 shows the first-order diffraction peaks of DMPC and DAPC close to T_M and several degrees above T_M. It is evident from the peak shapes, which are well reproduced by the model fits, that DMPC shows increased fluctuations as T_M is approached [Fig. 6(a)]. The increase of scattered intensity in the peak tails is clearly seen on the high-q side of the peaks. It is less clear, but also present on the low-q side of the peaks due to the modulation of the scattered intensity by the form factor. $|F(q)|^2$ approaches a minimum in this q regime and according to Eq. (1) suppresses the scattered intensity. This also gives the peak its asymmetric appearance and underlines the importance of considering the modulation of the form factor by the full q-range analysis. In contrast to DMPC, DAPC does not show an enhancement of the peak tails, when T_M is approached but a clear reduction of fluctuations [Fig. 6(b)].

The temperature dependencies of the bilayer undulations for all lipids studied are presented in Fig. 7. Starting at high

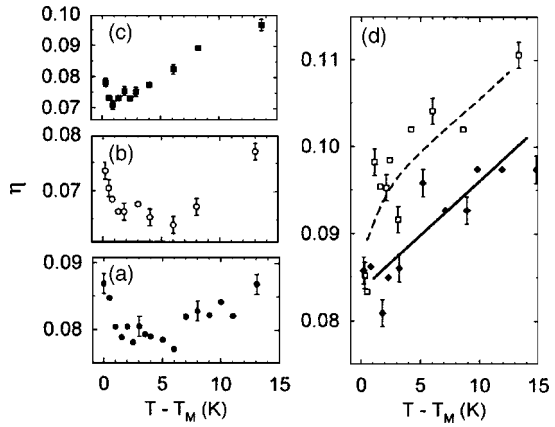

FIG. 7. Temperature dependence of the fluctuation parameter η for (a) DMPC (●), (b) DPPC (○), (c) DSPC (■), and (d) DNPC (□, dashed line) and DAPC (◆, solid line). Lines are drawn to guide the eye. All data presented in panels (a)–(c) show an increase of fluctuations in the vicinity of T_M, not observed in (d).

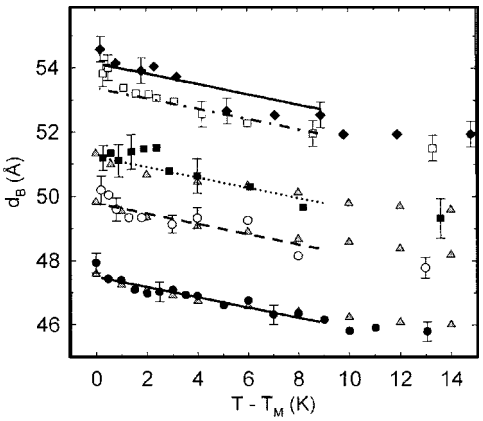

FIG. 8. Temperature dependence of the membrane thickness d_B for DMPC (●), DPPC (○), DSPC (■), DNPC (□), and DAPC (◆). The straight lines all have the same slope (~ -0.14 Å/K) determined from the DMPC data and show that the increment in d_B toward T_M is roughly the same for all lipids. Grey △'s show the corresponding temperature behavior of the d_C's determined from the first moment of DMPC-d_{54}, DPPC-d_{62}, and DSPC-d_{70} (data taken from Ref. [26]), appropriately scaled to the corresponding d_B data (see text).

temperatures DMPC, DPPC, and DSPC first show a decrease of η and then a sudden increase close to T_M [Figs. 7(a)–7(c)]. This increase in fluctuations is not found for the 19 and 20 carbons/chain lipids. Instead, η decreases for both lipids continuously as T_M is approached [Fig. 7(d)]. These results confirm our analysis of the water layer thickness (Fig. 5) [57]. The increase of η appears closer to T_M than the increase of d_W. This is due to the analysis applied, which is less sensitive to changes in bending fluctuations than to changes in structural parameters [21]. Hence, the increase of η can be detected only when fluctuations are most pronounced, i.e., just above the phase transition.

The increase of fluctuations can be directly attributed to a sudden drop in bending rigidity K_c causing a reduction of the bilayer interaction parameter B [21]. Both parameters are directly related to η by $(K_cB)^{-1/2}$. The decrease of K_c has also been estimated from the evolution of the thermal heat capacity [34], shape fluctuation analysis of giant unilamellar vesicles [33], an all-optical force method [35], and most recently by neutron reflectivity on a two-bilayer system [58].

Most interestingly, the last study also reports a reduction of K_c for DNPC and DAPC, for which we do not observe an increase of fluctuations. The reason might be that for longer-chain lipids the reduction of K_c has a smaller impact than for lipids with shorter chains. The bending rigidity of lipids generally increases with chain length [59], which in turn suppresses bending fluctuations for the longer-chain lipids. Further, the van der Waals attractions also and therefore the coupling between adjacent bilayers increase with chain length [60]. This again may suppress the increase of undulations in the vicinity of T_M.

C. Bilayer thickness

We now turn to the temperature dependence of the membrane thickness. Results are presented in Fig. 8, all showing a gradual increase as T_M is approached from above. Additionally, all lipids exhibit a small nonlinear component in the very vicinity of the transition point. The linear increase is attributed to a continuous reduction of *trans-gauche* isomers, consistent with the picture of "freezing-out" of the hydrocarbon chains. Microscopic modeling has suggested that the nonlinear part reflects critical behavior in the chain stiffening process [31]. The d_B data are much more scattered compared to d, which is due to the higher uncertainties in this case. However, if one draws a straight line through the DMPC data exhibiting the least scatter and shifts the line vertically it is evident that all lipids follow approximately the same slope (Fig. 8). Thus, there is no significant change in the overall behavior of the bilayer thickness as the chain length is increased. Figure 8 additionally shows, in excellent agreement with our x-ray data, the temperature dependence of d_C determined from deuterium NMR measurements on perdeuterated DMPC, DPPC, and DSPC [26]. Similar agreement is found for NMR data on perdeuterated DMPC reported by Nagle *et al.* [16], as demonstrated previously [21]. The comparison to NMR data is based on the assumption that the slightly lower transition temperatures of the perdeuterated lipids are the only difference from the nondeuterated analogs.

d_c is obtained from the NMR data by applying [26]

$$d_C = n_{\mathrm{HC}} \times (1.25\ \text{Å})[0.5 + \sqrt{3}M_1/(\pi 167\ \text{kHz})], \qquad (8)$$

where n_{HC} is the number of hydrocarbons per chain and M_1 the first moment of the NMR spectra reported by Morrow *et al.* [26]. Finally, a constant is added to the $2d_c$ values in order to obtain the best overall agreement to the d_B data reported in Fig. 8. For the individual lipids this constant varied between 20 and 22 Å, which is on the order of double the steric headgroup size for PCs [48]. Note that this simple procedure does not consider that in general chains may not be terminating at the center of the bilayer [61]. However, the good agreement between the two data sets justifies its usage.

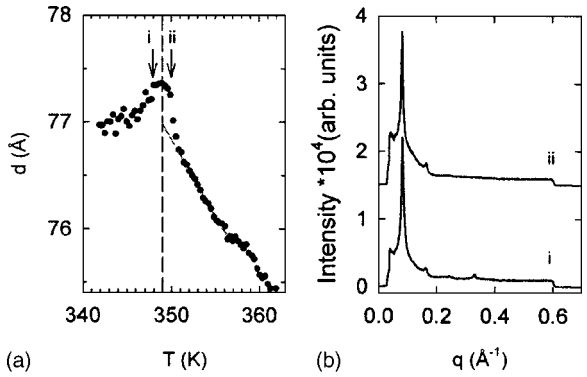

FIG. 9. (a) Temperature dependence of the d value of DBPC in the vicinity of the main phase transition (T_M=349 K). DBPC exhibits no ripple phase, but a gel phase of lamellar order as evidenced by the diffraction patterns (i) taken about 1.5 K below T_M (b). The diffraction pattern (ii) shows the system about 1 K above T_M in the L_α phase.

The NMR data therefore support our finding that d_B decreases for all lipids with temperature in a similar fashion (Fig. 8). Additionally, since the NMR data exhibit less scatter than the d_B's we may use them to get a better estimate of the nonlinear bilayer thickening component, which turns out to be about 0.5 Å, irrespective of the chain length. This agrees well with the Δd_{an}'s for DNPC and DAPC (Fig. 4), for which no NMR data are available. Combining all the evidences presented, we therefore conclude that the relative temperature dependence of d_B is the same for all lipids. Consequently, the anomalous swelling for DNPC and DAPC is exclusively due to the bilayer behavior. This is in agreement with both the absence of increased fluctuations [Fig. 7(d)] and a nearly unaltered bilayer separation [Fig. 5(d)] just above T_M.

In order to further confirm that the swelling for long lipids ($n_{\mathrm{HC}}>18$) is attributed solely to the increase in membrane thickness, we have performed a temperature scan (0.5 K/min) on DBPC [62]. Clearly, the d spacing increases nonlinearly as T_M is approached from above (Fig. 9). The anomalous component Δd_{an} is about 0.5 Å and therefore of the same magnitude as the residual swelling of DNPC and DAPC and further also as that for the bilayer component determined from NMR measurements [16,26].

We therefore arrive at the following picture of anomalous swelling. Below 18 hydrocarbons per chain the nonlinear increase of d in the vicinity of T_M is dominated by the expansion of the water layer. The contribution of d_W decreases with chain length and finally vanishes above 18 hydrocarbons per chains. For PCs with longer chains, the swelling is due to a nonlinear thickening of the bilayer, whose temperature behavior does not depend on the lipid chain length.

The constant 0.5 Å nonlinear component of d_B is difficult to rationalize. Is it truly critical and understandable in terms of a theory for hydrocarbon chain melting [31]? If it is critical, then we might expect the nonlinear contribution to increase as the chain length decreases, because the main transition of short-chain lipids was reported to be more critical-like than those of lipids with longer chains [14,26,29]. The nonlinear amplitude of d_B, however, does not show this behavior.

TABLE I. Chain-length dependence of the stable ripple phase cell parameters of fully hydrated DMPC (296.7 K), DPPC (312 K), and DAPC (338 K). The length of the long ripple λ_L, the short ripple λ_S, and its amplitude A have been estimated from the electron density maps presented in Fig. 10. γ is the angle between the vectors **a** and **b** of the 2D monoclinic unit cell, given by Eq. (4).

	a (Å)	b (Å)	γ (°)	λ_L (Å)	λ_S (Å)	A (Å)
DMPC	117.4	66.9	91.7	75	44	10
DPPC	136.8	72.1	95.3	100	42	13
DAPC	178.3	87.0	101.8	139	45	20

Does this mean that the membrane behavior in the vicinity of T_M is "normal," further implying that the main phase transition of PCs can be described in terms of a weakly first-order transition [30]? Not necessarily. Density fluctuations in one monolayer will in general not be correlated with the density fluctuations in the opposing membrane leaflet. This may then give, on the average over time and space of the measurement, no measurable contribution to a critical or pseudocritical membrane thickening.

D. Possible link to formation of ripple phase structure

It has been proposed that the hydration dynamics caused by pretransitional swelling are associated with the formation of the ripple phase [17]. It could be argued that this results from a freezing out of the thermal undulations, leading to a correlation of the fluctuations in the form of the rippled structure [20]. This scenario has been disproved by Mason *et al.* [20], who reported that monomethyl and dimethyl dimyristoyl phosphatidylethanolamine exhibit no ripple phase, but show pretransitional swelling.

This led us to test whether the previous findings extend to a different set of lipids. We have therefore determined the crystallographic parameters (Table I) and form factors (Table II) of fully hydrated DMPC and DAPC in the ripple phase at 296.7 K and 338 K, respectively. Here, the focus is on the ripple amplitude A and whether there is any correlation with the fluctuation amplitude above T_M, which is a function of the bilayer separation [60]. A recent study has reported little dependence of A on temperature [8]. Therefore, the actual temperature within the ripple phase and its relative value

TABLE II. Crystallographic data on indices and form factors of fully hydrated DMPC, DPPC, and DAPC. DPPC data taken from Ref. [50].

h	k	F_{hk}^{DMPC}	F_{hk}^{DPPC}	F_{hk}^{DAPC}
1	0	+0.9	+1.1	
0	1	+10.0	+10.0	+10.0
1	−1	−2.1	−2.5	−2.9
1	1	+1.9	+6.0	+8.9
0	2	−9.7	−7.1	−4.7
1	−2		+3.5	+4.2
1	2	−8.7	−8.0	−10.6

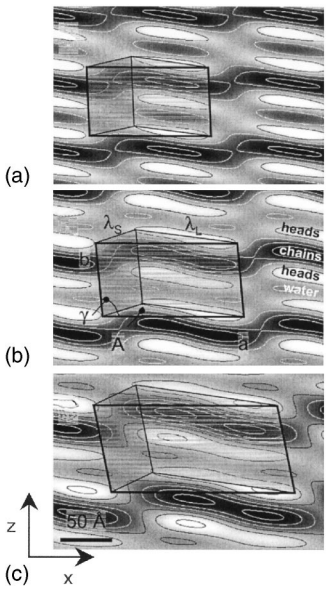

FIG. 10. Chain-length dependence of the stable ripple phase of DMPC (a), DPPC (b), and DAPC (c). The electron density is highest (white) for the phospholipid headgroup region and lowest (black) for the hydrocarbon chains. All electron density maps are presented on the same length scale.

with respect to T_M are of minor significance. Tables I and II also contain data for fully hydrated DPPC at 312 K taken from Rappolt and Rapp [50]. The EDMs (Fig. 10) have been calculated applying the form factors listed in Table II. It is evident from Table I and Fig. 10 that the cell parameters increase with chain length. Most important in the present context is, however, the observation that the ripple amplitude of DAPC is about twice the corresponding value for DMPC.

The data therefore show no correlation with the bending fluctuations in the L_α phase. From the latter we would expect that A either shows no trend with respect to n_{HC} because neither does the absolute value of d_W, or decreases with increasing chain length because of the reduction of the water layer swelling (Fig. 5). The results thus confirm the previous conclusion by Mason and co-workers [20] that the formation of the $P_{\beta'}$ phase is independent of anomalous swelling in the L_α phase.

There is additional evidence for this notion if we return to the original proposal by Richter *et al.* [17], which emphasized that the "bilayer hydration" caused by anomalous swelling could be the cause of the formation of the ripple phase. We have shown that, although all bilayers studied exhibit pretransitional swelling, the expansion of the water layer in the vicinity of T_M vanishes above 18 hydrocarbons per chain. Thus, in the explicit case of DAPC, there is no water layer swelling (Fig. 5) above T_M, while the system exhibits a ripple phase below T_M (Fig. 10) [63]. This is complementary to Ref. [20], which demonstrated pretransitional swelling in the absence of the formation of a ripple phase.

IV. SUMMARY AND CONCLUSION

We have analyzed the diffraction patterns of fully hydrated liposomal dispersions as a function of chain length and temperature above and below T_M. We have particularly focused on the temperature dependence of the structural parameters and the bilayer bending fluctuation in the vicinity of the fluid-to-gel transition. Additionally, the fully hydrated ripple phase structures of DMPC and DAPC have also been derived. The results are summarized as follows.

(1) All lipids studied exhibit anomalous swelling. The amplitude of the swelling decreases with increasing length of the hydrocarbon chains in agreement with Korreman and Posselt [18]. It does not vanish completely, however. Above 18 carbons per chain, it levels off and exhibits some residual swelling on the order of 0.5 Å.

(2) For $n_{\mathrm{HC}}<19$, the anomalous swelling is dominated by increased bending fluctuations and an expansion of the water layer in the vicinity of T_M. This contribution is reduced with increasing chain length and is not present for $n_{\mathrm{HC}}>18$.

(3) The second contribution to anomalous swelling is due to a nonlinear thickening of the lipid bilayer. While d_B increases with chain length, due to the additional hydrocarbon segments, its temperature dependency including the nonlinear component does not show significant changes. Therefore, the residual swelling for $n_{\mathrm{HC}}>18$ is due to the bilayer only.

(4) The amplitudes of the ripple phases increase with chain length and show no correlations with the chain-length dependencies of the absolute values of d_W or its relative increase close to T_M in the L_α phase. Further, DAPC and DNPC [63] exhibit a ripple phase in the absence of a pretransitional expansion of the water layer. This is complementary to the case demonstrated by Mason *et al.* [20]. Thus, there is no direct coupling between anomalous swelling and the formation of a ripple phase.

ACKNOWLEDGMENTS

We would like to thank W. Helfrich, J. Katsaras, and V. A. Raghunathan for many helpful discussions. This work has been supported by the European Union Grant No. INTAS-01-0105.

[1] M. J. Janiak, D. M. Small, and G. G. Shipley, Biochemistry **15**, 4575 (1976).
[2] D. C. Wack and W. W. Webb, Phys. Rev. A **40**, 2712 (1989).
[3] W. J. Sun, S. Tristram-Nagle, R. M. Suter, and J. F. Nagle, Proc. Natl. Acad. Sci. U.S.A. **93**, 7008 (1996).
[4] K. Sengupta, V. A. Raghunathan, and J. Katsaras, Europhys. Lett. **49**, 722 (2000).
[5] M. Rappolt, G. Pabst, G. Rapp, M. Kriechbaum, H. Amenitsch, C. Krenn, S. Bernstorff, and P. Laggner, Eur. Biophys. J. **29**, 125 (2000).
[6] See, for example, T. Heimburg, Biophys. J. **78**, 1154 (2000), and references therein.

[7] H. Yao, S. Matuoka, B. Tenchov, and I. Hatta, Biophys. J. **59**, 252 (1991).
[8] K. Sengupta, V. A. Raghunathan, and J. Katsaras, Phys. Rev. E **68**, 031710 (2003).
[9] K. Jørgensen, Biochim. Biophys. Acta **1240**, 111 (1995).
[10] K. Pressl, K. Jørgensen, and P. Laggner, Biochim. Biophys. Acta **1325**, 1 (1997).
[11] S. Kirchner and G. Cevc, Europhys. Lett. **23**, 229 (1993).
[12] T. Hønger, K. Mortensen, J. H. Ipsen, J. Lemmich, R. Bauer, and O. G. Mouritsen, Phys. Rev. Lett. **72**, 3911 (1994).
[13] R. Zhang, W. Sun, S. Tristram-Nagle, R. L. Headrick, R. M. Suter, and J. F. Nagle, Phys. Rev. Lett. **74**, 2832 (1995).
[14] J. Lemmich, K. Mortensen, J. H. Ipsen, T. Hønger, R. Bauer, and O. G. Mouritsen, Phys. Rev. Lett. **75**, 3958 (1995).
[15] F. Y. Chen, W. C. Hung, and H. W. Huang, Phys. Rev. Lett. **79**, 4026 (1997).
[16] J. F. Nagle, H. I. Petrache, N. Gouliaev, S. Tristram-Nagle, Y. F. Liu, R. M. Suter, and K. Gawrisch, Phys. Rev. E **58**, 7769 (1998).
[17] F. Richter, L. Finegold, and G. Rapp, Phys. Rev. E **59**, 3483 (1999).
[18] S. S. Korreman and D. Posselt, Eur. Phys. J. E **1**, 87 (2000).
[19] S. S. Korreman and D. Posselt, Eur. Biophys. J. **30**, 121 (2001).
[20] P. C. Mason, J. F. Nagle, R. M. Epand, and J. Katsaras, Phys. Rev. E **63**, 030902 (2001).
[21] G. Pabst, J. Katsaras, V. A. Raghunathan, and M. Rappolt, Langmuir **19**, 1716 (2003).
[22] D. Papahadjopoulos, K. Jacobson, S. Nir, and T. Isac, Biochim. Biophys. Acta **311**, 330 (1973).
[23] J. F. Nagle and H. L. Scott, Biochim. Biophys. Acta **513**, 236 (1978).
[24] I. Hatta, K. Suzuki, and S. Imaizumi, J. Phys. Soc. Jpn. **52**, 2790 (1983).
[25] A. Ruggiero and B. Hudson, Biophys. J. **55**, 1111 (1989).
[26] M. R. Morrow, J. P. Whitehead, and D. Lu, Biophys. J. **63**, 18 (1992).
[27] D. P. Kharakoz, A. Colotto, K. Lohner, and P. Laggner, J. Phys. Chem. **97**, 9844 (1993).
[28] E. Freire and R. Biltonen, Biochim. Biophys. Acta **514**, 54 (1978).
[29] J. H. Ipsen, K. Jørgensen, and O. G. Mouritsen, Biophys. J. **58**, 1099 (1990).
[30] D. P. Kharakoz and E. A. Shlyapnikova, J. Phys. Chem. B **104**, 10368 (2000).
[31] J. F. Nagle, Annu. Rev. Phys. Chem. **31**, 157 (1980).
[32] O. G. Mouritsen, Chem. Phys. Lipids **57**, 179 (1991).
[33] L. Fernandez-Puente, I. Bivas, M. D. Mitov, and P. Méléard, Europhys. Lett. **28**, 181 (1994).
[34] T. Heimburg, Biochim. Biophys. Acta **1415**, 147 (1998).
[35] C. H. Lee, W. C. Lin, and J. Wang, Phys. Rev. E **64**, 020901 (2001).
[36] W. Helfrich, Z. Naturforsch. A **33a**, 305 (1978).
[37] T. A. Harroun, M. P. Nieh, M. J. Watson, V. A. Raghunathan, G. Pabst, M. R. Morrow, and J. Katsaras, Phys. Rev. E **69**, 031906 (2004).
[38] H. Amenitsch, M. Rappolt, M. Kriechbaum, H. Mio, P. Laggner, and S. Bernstorff, J. Synchrotron Radiat. **5**, 506 (1998).
[39] S. Bernstorff, H. Amenitsch, and P. Laggner, J. Synchrotron Radiat. **5**, 1215 (1998).
[40] A. M. Petrascu, M. H. J. Koch, and A. Gabriel, J. Macromol. Sci., Phys. **B37**, 463 (1998).
[41] G. Pabst, M. Rappolt, H. Amenitsch, and P. Laggner, Phys. Rev. E **62**, 4000 (2000).
[42] T. C. Huang, H. Toraya, T. N. Blanton, and Y. Wu, J. Appl. Crystallogr. **26**, 180 (1993).
[43] R. Zhang, R. M. Suter, and J. F. Nagle, Phys. Rev. E **50**, 5047 (1994).
[44] H. I. Petrache, Ph.D. thesis, Carnegie Mellon University, 1998.
[45] G. Pabst, R. Koschuch, B. Pozo-Navas, M. Rappolt, K. Lohner, and P. Laggner, J. Appl. Crystallogr. **63**, 1378 (2003).
[46] A. Caillé, C. R. Seances Acad. Sci., Ser. B **274**, 891 (1972).
[47] J. F. Nagle and S. Tristram-Nagle, Biochim. Biophys. Acta **1469**, 159 (2000).
[48] T. J. McIntosh and S. A. Simon, Biochemistry **25**, 4058 (1986).
[49] J. Katsaras, S. Tristram-Nagle, Y. Liu, R. L. Headrick, E. Fontes, P. C. Mason, and J. F. Nagle, Phys. Rev. E **61**, 5668 (2000).
[50] M. Rappolt and G. Rapp, Eur. Biophys. J. **24**, 381 (1996).
[51] A. Tardieu, V. Luzzati, and F. C. Reman, J. Mol. Biol. **75**, 711 (1973).
[52] B. E. Warren, *X-ray Diffraction* (Addison-Wesley, Reading, MA, 1969).
[53] V. Luzzati, P. Mariani, and H. Delacroix, Makromol. Chem., Macromol. Symp. **15**, 1 (1988).
[54] G. Pabst, J. Katsaras, and V. A. Raghunathan, Phys. Rev. Lett. **88**, 128101 (2002).
[55] In the absence of an analytical model that distinguishes between normal and abnormal components of the swelling, the given Δd_{an}'s are certainly only rough figures. The applied method is, however, sufficient to determine the overall chain-length dependence of the anomalous swelling component.
[56] The magnitude of pretransitional swelling is affected only if the system is significantly dehydrated [21].
[57] η shows the same nonmonotonic variation with n_{HC} as d_W. This is due to the functional dependence of η on the interbilayer compressional modulus, which in turn depends on the bilayer separation.
[58] G. Fragneto, T. Charitat, E. Bellet-Amalric, R. Cubitt, and F. Graner, Langmuir **19**, 7695 (2003).
[59] E. Evans, Biophys. J. **14**, 923 (1974).
[60] R. Lipowsky, in *Structure and Dynamics of Membranes*, edited by R. Lipowsky and E. Sackmann (North-Holland, Amsterdam, 1995).
[61] J. F. Nagle, Biophys. J. **64**, 1476 (1993).
[62] The decompsition of d into d_W and d_B is not possible in this case because of shorter x-ray exposure times (10 s).
[63] The same is found for DNPC, which is known to exhibit a ripple phase [R. Koynova and M. Caffrey, Biochim. Biophys. Acta **1376**, 91 (1998)], but for which we have not determined the ripple structure.